Integrating Wavelet Empirical Orthogonal Functions and Statistical Disaggregation for Predicting Weekly Runoff for the Upper Kafue Basin in Zambia, Africa

Davison Mwale[1] and Thian Yew Gan, F.ASCE[2]

Abstract: Wavelet empirical orthogonal function analysis, genetic algorithm driven neural networks, statistical disaggregation and hydrologic modeling were integrated into a hydrologic framework to predict weekly rainfall and runoff of the upper Kafue and Lunga Rivers in Zambia, Africa. The April–June (AMJ) seasonal variability of the Atlantic Ocean, on the basis of its AMJ sea surface temperatures, was used to predict the annual rainfall of two stations, Ndola in the upper Kafue River Basin and Solwezi in the Lunga River Basin. The predicted annual rainfall at the two stations was disaggregated to weekly totals and then used to simulate the runoff of the upper Kafue and Lunga Rivers. In the upper Kafue basin, runoff from the disaggregated weekly rainfall explained 81% of the runoff variance, compared to 88% when historical weekly rainfall data was used. For the Lunga River, 72% of the observed runoff variance was accounted for, compared to 81% when historical weekly rainfall was used. This scheme demonstrates that if a region is dominated by hydro-climatic processes whose statistics are fairly stationary, it will be possible to use disaggregated rainfall from annual rainfall predicted by a teleconnection model to predict reliable weekly basin runoff up to a year's lead time useful for an integrated water resources management.

DOI: 10.1061/(ASCE)HE.1943-5584.0000231

CE Database subject headings: Wavelet; Empirical equation; Statistics; Hydrologic models; River basins; Zambia; Africa; Runoff; Water resources.

Author keywords: Wavelet empirical orthogonal function analysis; Genetic algorithm-neural network; Statistical disaggregation; Hydrologic modeling; Kafue River Basin; Zambia.

Introduction

Between 1965 and the late 1990s, parts of southern Africa, especially regions north of 25°S experienced gradual but consistent decrease in rainfall (Mwale et al. 2007). The reduction in rainfall resulted in the decrease of runoff for many rivers in the region (Fanta et al. 2001). The considerable imbalance between water supply and demand, which became noticeable in the 1990s (Jury and Engert 1999), forced regional governments to call for the development of legal and political frameworks to manage the declining local and regional water resources in a holistic way (*The Water Page* 2005). While legal and political frameworks form cornerstones of integrated water resources management, sound hydrologic frameworks, which design efficient and sustainable solutions to solving water resources problems, are required to ensure an integrated management of water resources. Hydrologic frameworks complement legal and political frameworks by integrating knowledge of the dominant spatial, temporal and frequency regimes of climatic and hydrologic variability and their predictability into various levels of integrated water resources management.

One region that could benefit from such a holistic water resource management framework is the Kafue River Basin, located in central Zambia, Africa (Fig. 1). This river basin provides water to more than 40% of Zambia's population, supplies part of the country's hydroelectric power generation, provides municipal water supply to the Copper-belt and Lusaka provinces, meets the irrigation demand of the Nakambala sugar estate located south of the capital of Lusaka, and provides water for wildlife in the Kafue National Park.

To implement the hydrologic framework, basin scale hydrologic models (e.g., Bindlish and Baros 2000; Kerkhoven and Gan 2006) which can simulate hourly, daily, or weekly streamflow from predicted precipitation at hourly, daily, or weekly time scales with lead times of three months or more will be necessary. Ideally, partly to consider feedbacks between land and atmosphere, streamflow could be simulated using fully distributed hydrologic models coupled to general circulation models or mesoscale atmospheric models. Atmospheric models could simulate precipitation fields at hourly or daily time steps for the com-

[1]State of Delaware, Department of Natural Resources and Environmental Control, Financial Assistance Branch, 5 E. Reed Street, Dover, DE 19901.

[2]Civil and Environmental Engineering, University of Alberta, Edmonton, Alberta, Canada T6G 2W2. Email: tgan@ualberta.ca

Note. This manuscript was submitted on March 7, 2008; approved on February 8, 2010; published online on February 17, 2010. Discussion period open until March 1, 2011; separate discussions must be submitted for individual papers. This paper is part of the ***Journal of Hydrologic Engineering***, Vol. 15, No. 10, October 1, 2010. ©ASCE, ISSN 1084-0699/2010/10-822–833/$25.00.

Downloaded 29 Dec 2010 to 160.36.192.127. Redistribution subject to ASCE license or copyright. Visit http://www.ascelibrary.org

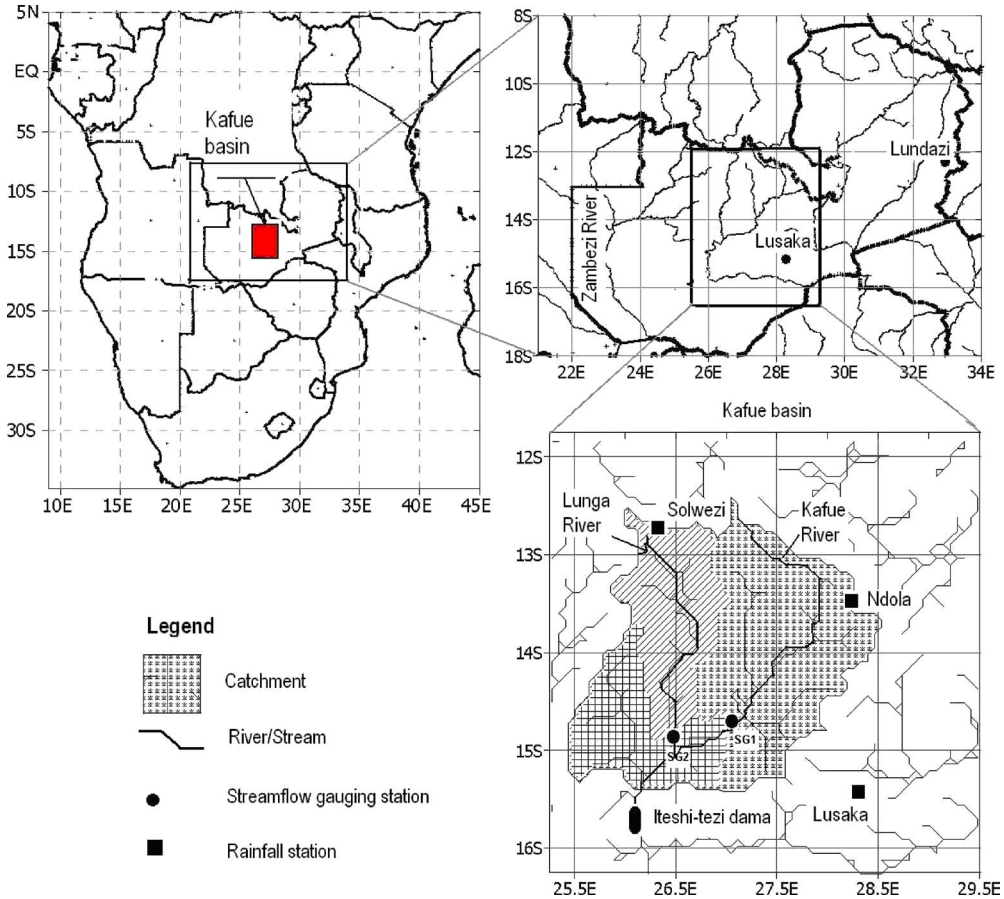

Fig. 1. Location of the study area. The upper Kafue River Basin is denoted with stars and Lunga River Basin is hatched. Their gauging locations are shown as SG1 for the upper Kafue River and SG2 for the Lunga River. The rainfall gauging stations for the Lunga and Kafue River Basins are at Solwezi and Ndola, respectively. Both rivers drain into the Iteshi-Teshi Dam.

ing rainy season and their output could then be used to drive hydrologic models (Yarnal et al. 2000). However, numerical atmospheric models generally have problems forecasting accurate climate data beyond a week because of chaos or round-off errors (Peitgen et al. 1992). Therefore, for streamflows prediction at seasonal scale, coupling a hydrologic with atmospheric models may not lead to meaningful results for the Kafue River Basin.

In other words, instead of coupled climatic-hydrologic modeling, a more modest but practical approach would be to integrate statistical methods with a lumped parameter hydrologic model. Statistical methods can predict annual rainfall with lead times of three months or more which can be disaggregated into smaller time scales suitable for driving a conceptual, lumped hydrologic model to simulate the streamflow of a river basin. If meaningful rainfall and streamflow prediction can be achieved at a seasonal to a year's lead time, the proposed hydrologic framework can be a useful tool especially during periods of prolonged droughts. The disaggregation of seasonal rainfall of the Kafue River Basin may be carried out using the approaches by Valencia and Schaake (1973) and the analog approach by Lorenz (1969). In using the analog approach long data sets are required so that many similar episodes of weekly, monthly and annual aggregates can be found in the observations. Since the Kafue River Basin has only limited hydro-climatic data, only the disaggregation method of Valencia and Schaake (1973) could be used.

The objective of this study is to develop a hydrologic framework that integrates wavelet empirical orthogonal analysis, statistical disaggregation, genetic algorithm-neural networks and a lumped parameter, hydrologic model, to predict the weekly runoff of the Kafue River Basin at a seasonal, and possibly up to a year lead time.

Study Site and Data

Kafue River Basin

The Kafue River Basin has a total area of 157,000 km^2, is located on the central African plateau approximately between 12.5–17°S and 25.5–29.5°E, and lies completely within central Zambia (see Fig. 1) (United Nations Development Planning/Food and Agricultural Organization/Government of the Republic of Zambia, 1968 report or UNDP/FAO/GRZ 1968). The river basin can be divided into three zones: the upper Kafue basin, which extends from the head waters to the Iteshi-Teshi Dam; the middle Kafue basin, which extends from the Iteshi-Teshi Dam to the Kafue Gorge Dam; and the lower Kafue basin, which extends from the Kafue Gorge to the Zambezi River confluence. The eastern part of the upper Kafue River Basin is dominated by the Lukanga swamps, where most rivers to the east of the basin drain into. Hence, the effective area contributing to the upper Kafue River stream flow is only 34,162 km^2, while that to the Lunga River is 24,268 km^2.

The upper reaches of the Kafue River Basin are dominated by clays and sands, each accounting for between 30–40% of the

Downloaded 29 Dec 2010 to 160.36.192.127. Redistribution subject to ASCE license or copyright. Visit http://www.ascelibrary.org

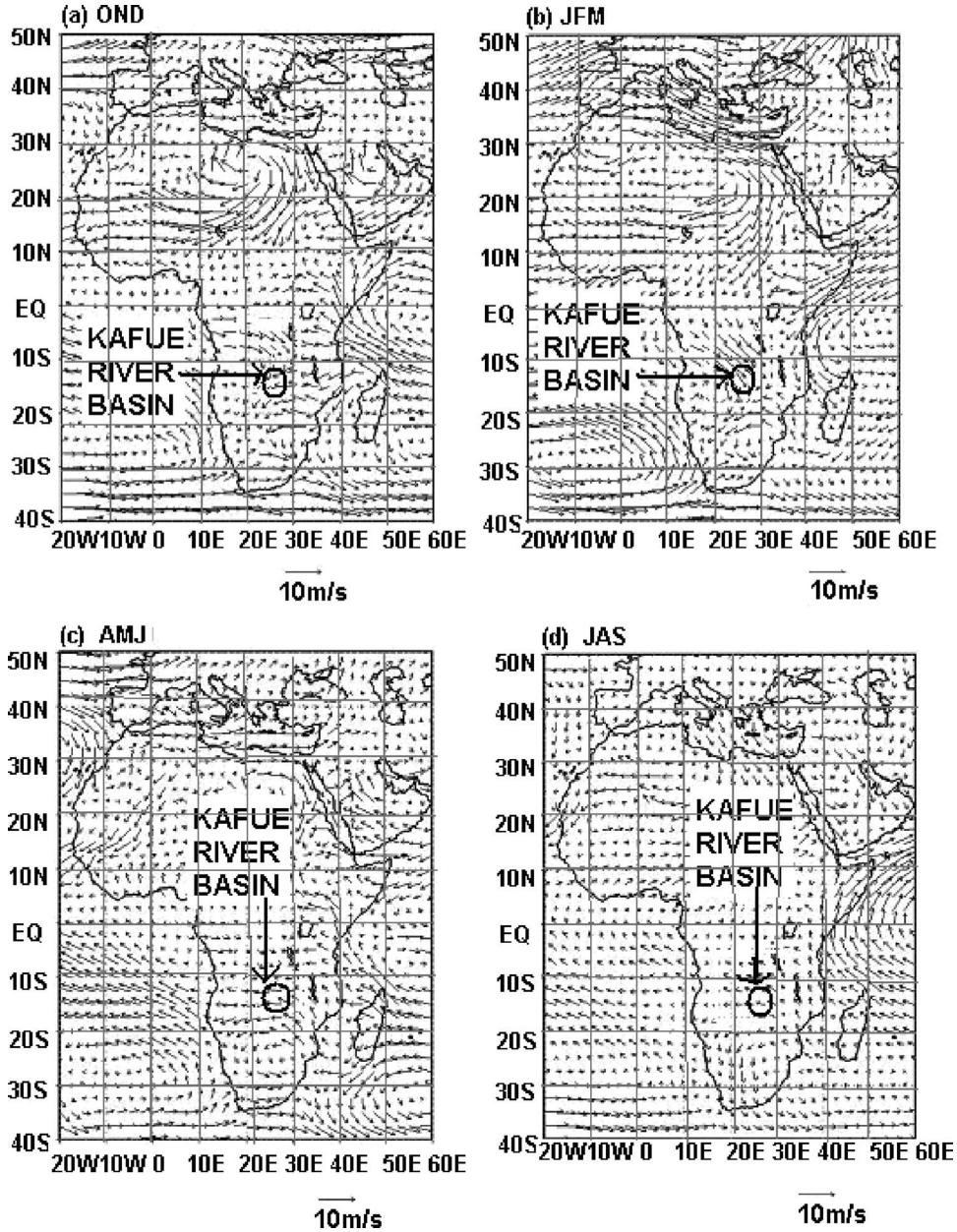

Fig. 2. 850-hPa winds showing the prevailing atmospheric circulation and moisture transport in terms of wind speed (m/s) and direction for the months of (a) OND; (b) JFM; (c) AMJ; and (d) JAS

soil type, while in the middle and eastern sections, sandy soils account for 40–50% of the soil types (figures not shown). There are also many saucepan-shaped depressions, called "Dambos," which are seasonally waterlogged (UNDP/FAO/GRZ 1968). As a result, during wet years considerable Horton overland flow occurs, while during dry years the detention storage of these Dambos dominates the water budget, resulting in little surface runoff. Tropical grasslands and trees are also a dominant feature of the basin. During summer in the Southern Hemisphere (SH) (September–November), the temperature of Kafue is generally high while during winter (June–July), its temperature is low, but for the rest of the year, mild temperature dominates.

Existing Climatic Regime

The Kafue River Basin is characterized by a rainfall regime driven by the October–March (summer in the SH) inflow of the moist Congo air mass into the basin (Fig. 2), and the March–April outflow of the Congo air mass from the basin. The SH summer causes low pressures to develop in the Kafue basin, drawing in the Congo air mass and causing wide spread rains (UNDP/FAO/GRZ 1968). The air mass flows out of the basin between March 31 and April 25, bringing an end to the rainfall season (UNDP/FAO/GRZ 1968). Statistical properties from the fairly consistent climatic regime were used to generate future rainfall at time steps that are fine enough to drive a properly calibrated lumped parameter rainfall-runoff model, which was then used to predict the runoff hydrographs of the Kafue basin for the coming water year.

Available Data

Daily natural streamflow data (m^3/s) for the upper Kafue River was available from 1962 to 1988, and for the Lunga River from 1962 to 1982. Both data sets in m^3/s were converted to mm/day

Downloaded 29 Dec 2010 to 160.36.192.127. Redistribution subject to ASCE license or copyright. Visit http://www.ascelibrary.org

by normalizing the streamflow of each river by its drainage area. The daily runoff was summed to weekly, monthly and annual totals. Daily rainfall data from 1962 to 1988 was taken from two rainfall stations, Ndola and Solwezi, located at the upper reaches of the basin. The daily rainfall at Ndola and Solwezi were converted to weekly, monthly, seasonal (i.e., October–December (OND), January–March (JFM), April–June (AMJ) and July–September (JAS)) and annual values. Monthly rainfall data, gridded at a resolution of 2.5° lat.×3.75° long., was also extracted for central southern Africa (CSA) (6°S-18°S, 13°E-36°E). Gridded monthly sea surface temperature (SST) for 1950–1997, at 5°×5° resolution for the south Atlantic (10°N-40°S, 55°W-10°E) and the Indian Oceans (20°N-40°S and 40°E-105°E) (figures not shown), were provided by the U.K. meteorological office. Monthly air temperature data of 1950–1998 was obtained from the SAFARI 2000 project (New et al. 2002) (http://www.daac.ornl.gov). The sunshine hours and relative humidity data were obtained from UNDP/FAO/GRZ (1968).

Research Procedure

The implementation of the Kafue River Basin hydrologic framework involved the following steps:

1. The wavelet empirical orthogonal function (WEOF) analysis was applied to the annual rainfall (ONDJFM) and the AMJ SST data to establish the spatial and temporal patterns of annual rainfall of the Kafue River Basin and AMJ SST variability of the Atlantic Ocean respectively (see Mwale and Gan 2005). WEOF was applied to the annual rainfall of the entire central southern Africa (CSA) region, which encompasses the Kafue River Basin, to establish the teleconnection between the variability of AMJ SST of the Atlantic Ocean and the dominant regional patterns of rainfall of an area (CSA) larger than the study site at Kafue. The AMJ SST of the Atlantic Ocean was chosen because it has been shown to teleconnect well with the rainfall of CSA at a 3-month lead time (Mwale et al. 2004);
2. Establish the teleconnection patterns between the annual rainfall of CSA and the AMJ Atlantic ocean SST variability;
3. Using the established SST teleconnection patterns in step (2), and part of the annual rainfall data collected from Ndola and Solwezi, calibrate the ANN-GA model. Then the remaining AMJ SST data was used to drive the calibrated ANN-GA model to validate its predicted annual rainfall at Ndola and Solwezi;
4. The predicted annual rainfall at Ndola and Solwezi was disaggregated to weekly rainfall totals; and
5. The disaggregated weekly rainfall at Ndola and Solwezi was used to drive a conceptual, lumped parameter, soil moisture accounting model (the Sacramento Model) to predict the weekly runoff of the upper Kafue River Basin.

Details of the above steps are given below.

Application of Wavelet Empirical Orthogonal Function

WEOF was applied to first transform the observed rainfall and SST time series, $O(t)$, by a mother wavelet, ψ, to a wavelet spectrum $W(b,a)$

$$W(b,a) = \frac{1}{\sqrt{a}} \int_0^T O(t) \Psi^* \left(\frac{t-b}{a} \right) dt \tag{1}$$

where ψ^*=complex conjugate of ψ; a =scale (or periodic cycle) of the wavelet; and b=translation position along the t-axis. At each scale, the wavelet spectra coefficients (also known as power or energy) depict how well the mother wavelet matches the observed rainfall or SST time series, $O(t)$. The quantity $a^{-1/2}$ in Eq. (1) is an energy normalization term to ensure that the energy of the mother and daughter wavelets remain the same over all scales, making it possible to directly compare wavelet transforms of one time series with another (Torrence and Compo 1998).

Next, the scale-averaged wavelet power (SAWP), which represents the mean variance of wavelet coefficients over a range of scales, was computed from the wavelet spectrum, to examine the variation of rainfall and SST over a range of statistically significant oscillations, as

$$W_t^2 = \frac{\delta_j \delta_t}{C_\delta} \sum_{j=j_1}^{j_2} \frac{|W_t(b,a_j)|^2}{a_j} \tag{2}$$

where C_δ=0.776 for the Morlet wavelet; δ_j=factor for scale averaging; and δ_t=sampling period (Torrence and Compo 1998). Since SAWP is a time series of average variance in a certain frequency band, SAWP can also be used to examine the modulation of one time series by another (e.g., variation of rainfall due to SST variations) or the modulation of one frequency by another within the same time series.

To determine the dominant spatial and temporal patterns of rainfall and SST and the teleconnection between these patterns, the empirical orthogonal function analysis was applied to the SAWP of rainfall and SST

$$\mathbf{u_m} = \mathbf{e_m^T x'} = \sum_{k=1}^{K} e_{km} x'_k, \quad m = 1, \ldots, M \quad (\text{where } M \ll K) \tag{3}$$

where $\mathbf{u_m}$=wavelet principle components (WPCs) time series of rainfall or SST SAWP; e_{km} (x'_k)=eigenvectors (anomalies) of the SAWP; and M represents the number of dominant WPCs that accounted for majority of the variability in the SAWP.

Then, the dominant spatial patterns of rainfall [Fig. 3(a)] and SST variability (figures not shown) were established by correlating the leading WPC of rainfall and SST (i.e., WPC1) to the gridded SAWP of rainfall and SST, respectively. Furthermore, teleconnection patterns between rainfall and SST were established by correlating the rainfall WPC1 and the SAWP of AMJ SST [see Fig. 3(b)].

Having established the spatial patterns shown in Fig. 3(b), the AMJ SST data to be used for training the genetic algorithm neural network (ANN-GA) model and for predicting the rainfall of Solwezi and Ndola were extracted from areas of the Atlantic Ocean [Fig. 3(b)] where the correlation exceeded 0.5.

ANN-GA for Predicting Annual Rainfall

The ANN-GA model of Mwale et al. (2004) (see Fig. 4) was trained to predict the annual rainfall at Ndola and Solwezi using AMJ SST data selected from the Atlantic Ocean as shown in Fig. 3(b). To train the best ANN-GA model for a given set of data, five procedures, "evaluation," "ranking," "selection," "crossover" and "mutation," of the genetic algorithm (GA) were applied to hundreds of thousands of artificial neural networks (ANNs) through hundreds of iterations called generations:

First, the ANN-GA randomly generates hundreds of neural networks called a population (Fig. 4). Each neural network in the population has three layers (i.e., input layer, middle layer and outer layer). The number of input layers depends on the number of AMJ SST data points chosen for training or predicting the

Downloaded 29 Dec 2010 to 160.36.192.127. Redistribution subject to ASCE license or copyright. Visit http://www.ascelibrary.org

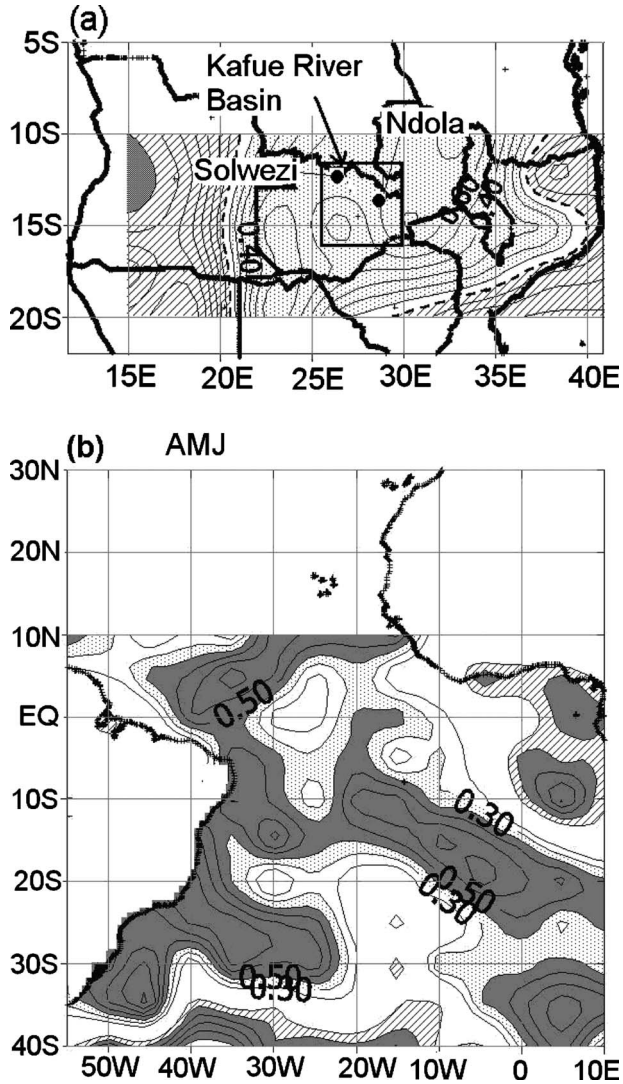

Fig. 3. Plots showing (a) the dominant spatial pattern of rainfall in central southern Africa that includes the Kafue River Basin; (b) areas of the Atlantic Ocean where April–June (AMJ) sea surface temperatures data was extracted to train the ANN-GA model and predict rainfall at Ndola and Solwezi

annual rainfall, the middle (hidden) layer contains three neurons and the output layer, which represents the annual rainfall to be predicted, has one neuron. Each layer has weights that translate the AMJ SST data from the input layer, through the middle layer to the outer layer. The translated AMJ SST data in the outer layer (as predicted annual rainfall) is then compared with the observed annual rainfall. Different metrics such as correlation, root mean square errors or Hansen Kuipers score could be used to compare the translated SST and the observed rainfall data. If the discrepancy between the translated SST and the observed rainfall data are large, the weights in all the layers are adjusted until a good agreement between them is achieved. In this study standardized rainfall and SST were used, and the agreement between the predicted and the observed annual rainfall was assessed in terms of correlation coefficient. The predicted rainfall in the standardized form was then multiplied with its standard deviation and added to its mean to become the actual rainfall.

Next, the ANNs are ranked according to how well their weights translated the SST data into annual rainfall. The best

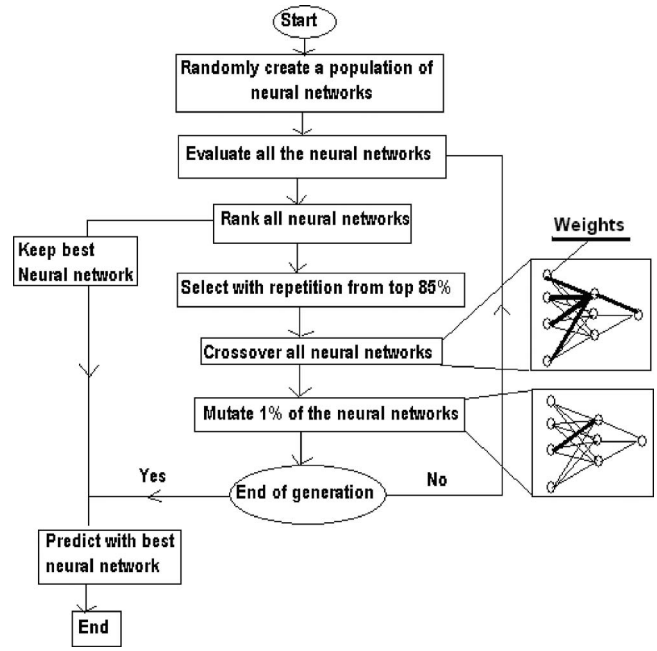

Fig. 4. ANN-GA model

ANN at each generation is put away separately and only replaced if a better ANN is found. To continue searching for a better ANN, the top 85% of the population are randomly selected to form another 100% of a new population. Since the selection is only taken from the top 85% of the population, some ANNs are selected more than once.

After the ANNs are selected, they undergo crossover whereby the weights between any two randomly selected ANNs are exchanged by randomly identifying a point in the middle layer and exchanging all weights on either side of the point (see Fig. 4). After crossover, a few ANNs are allowed to undergo mutation in which weights of a few selected ANNs are randomly altered. Usually only 1% of ANNs are randomly chosen from the population and a small portion of their weights are randomly altered. Similar to natural processes, mutation does not usually produce desirable traits in ANNs and hence it is applied sparingly.

At Ndola, the 1962–1983 annual rainfall and AMJ SST data were used for training the ANN-GA and the remaining data (1984–1988) was used to predict the 1984–1988 annual rainfall. At Solwezi, the 1962–1979 data were used to train the ANN-GA and then the 1980–1982 AMJ SST data was used to predict the 1980–1982 annual rainfall. Using the AMJ SST data of Fig. 3(b), the annual rainfall predicted for Ndola and Solwezi (shown in Figs. 5(a and b), respectively) were further disaggregated to weekly totals before being used to drive the SAC-SMA hydrologic model.

Statistical Disaggregation of Annual Rainfall

The total length of the upper Kafue River from the source to the gauging station (SG1 in Fig. 1) is about 410 km and has a slope of about 0.09%. For such natural channels, approximate average velocities range between 0 and 0.61 msecond^{-1} (Chow et al. 1988), which means that the time the entire watershed begins to contribute streamflow at the reservoir is 7.8 or about 8 days and so it is appropriate to disaggregate the seasonal rainfall into weekly time steps. Out of convenience, for months with 31 days, the stream flows for the first three weeks were averaged over

Downloaded 29 Dec 2010 to 160.36.192.127. Redistribution subject to ASCE license or copyright. Visit http://www.ascelibrary.org

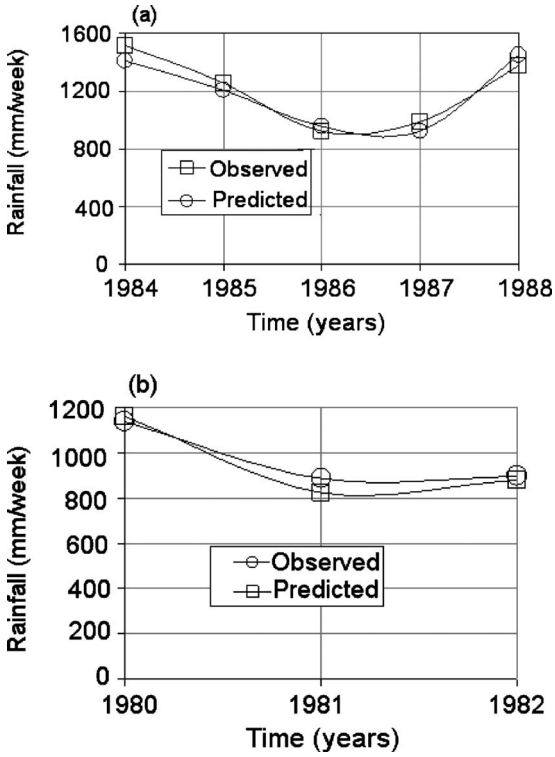

Fig. 5. Plots of the predicted and the observed annual rainfall at (a) Ndola; (b) Solwezi in the Kafue River Basin

eight days, while the stream flows for the last week was averaged over seven days. For months with 30 days, the first two weeks were averaged over eight days while the last two weeks over seven days. By so doing, we ended up with only forty eight (48) weeks per year, instead of fifty two (52) weeks.

In the first disaggregation stage, statistical properties between annual and monthly rainfall are used to disaggregate the annual rainfall into twelve (12) monthly rainfall totals (Fig. 6). Next the 12 annual monthly totals are aggregated to three month seasonal totals of OND, JFM, AMJ, and JAS. In the second stage, statistical properties between seasonal and weekly rainfall are used to disaggregate the seasonal rainfall into twelve weekly rainfall totals for each of the OND, JFM, AMJ and JAS seasons (i.e., for a total of 48 weekly rainfall totals).

The disaggregation of annual rainfall to 12 monthly totals or from each of the seasonal rainfall totals (OND, JFM, AMJ or JAS) to 12 weekly rainfall totals takes the following form:

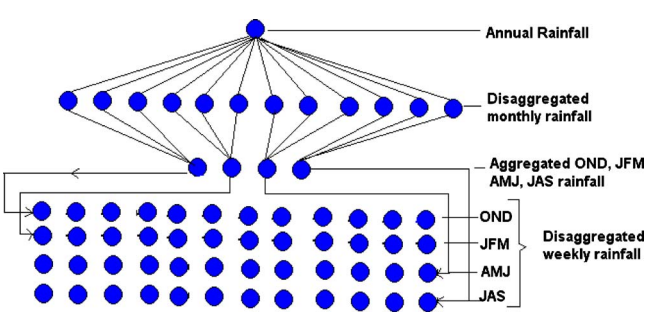

Fig. 6. Illustration of the disaggregation procedure

$$\mathbf{y}(\mathbf{t}) = \mathbf{d}\mathbf{x}(\mathbf{t}) + \mathbf{f}\mathbf{v}(\mathbf{t}) \tag{4}$$

where $\mathbf{y}(\mathbf{t})$ is a $k \times 1$ vector of 12 monthly (or 12 weekly) rainfall totals of year (season) t, k the number of months (weeks) in the year (season), $x(t)$ the annual (seasonal) rainfall for year (season) $\mathbf{t}$, $\mathbf{v}(\mathbf{t})$ is a $k \times 1$ vector of random standard normal deviates (with a mean zero and variance of one), $\mathbf{d}$ is a $k \times 1$ vector and $\mathbf{f}$ is a $k \times k$ matrix, of coefficients (Valencia and Schaake 1973). The elements of vector $\mathbf{d}$ sum to one and can be considered as monthly (weekly) contributions to the annual (seasonal) rainfall of vector $\mathbf{x}(\mathbf{t})$. The vector resulting from the product of matrix $\mathbf{f}$ and vector $\mathbf{v}(\mathbf{t})$ adds a random variation to $\mathbf{y}(\mathbf{t})$, so that $\mathbf{y}(\mathbf{t})$ reflects some degree of stochastic variability observed at weekly time steps. The vector $\mathbf{d}$ and matrix $\mathbf{f}$ are derived by analyzing historic rainfall data as follows:

$$\mathbf{d} = \mathbf{s}_{\mathbf{yx}}\mathbf{s}_{\mathbf{xx}}^{-1} \tag{5}$$

$$\mathbf{f}\mathbf{f}^T = \mathbf{s}_{\mathbf{yy}} - \mathbf{s}_{\mathbf{yx}}\mathbf{s}_{\mathbf{xx}}^{-1}\mathbf{s}_{\mathbf{xy}} \tag{6}$$

where the covariance matrices between different levels of aggregation (i.e., monthly and annual or seasonal and weekly) are denoted by $\mathbf{s}_{\mathbf{yx}}$ and $\mathbf{s}_{\mathbf{xy}}$, while variances by $\mathbf{s}_{\mathbf{xx}}$ and $\mathbf{s}_{\mathbf{yy}}$. The vector $\mathbf{d}$ is computed directly from Eq. (5) but there is no unique solution to the matrix $\mathbf{f}$ from $\mathbf{f}\mathbf{f}^T$ given in Eq. (6). Matrices of the form $\mathbf{f}\mathbf{f}^T = \mathbf{c}$ are called Gramian matrices, $\mathbf{c}$ being the Gramian of $\mathbf{f}$. Given c there is no unique solution to $\mathbf{f}$ since any matrix of the form $\boldsymbol{f}.\mathbf{e}$, where $\mathbf{e}$ is orthogonal, will satisfy the above relationship. The necessary and sufficient condition for estimating $\mathbf{f}$ is that the covariance structure of $\mathbf{c}$ be positive semi-definite, as shown by Valencia and Schaake (1972). The most common method used to estimate $\mathbf{f}$ is the empirical orthogonal function factorization. By equating the Gramian matrix $\mathbf{c}$, to the left hand side of Eq. (6)

$$\mathbf{f}\mathbf{f}^T = \mathbf{c} \tag{7}$$

The eigenvector solution of Eq. (7) is

$$\mathbf{c}\mathbf{e} = \mathbf{e}\lambda \tag{8}$$

where λ_i are the eigenvalues and $\mathbf{e}$ the eigenvectors that are orthogonal to each other. Multiplying both sides of Eq. (8) by e^{-1}, we obtain

$$\mathbf{c} = \mathbf{e}\lambda\mathbf{e}^{-1} = \mathbf{f}\mathbf{f}^T \tag{9}$$

which reduces to

$$\mathbf{f} = \mathbf{e}\boldsymbol{\lambda}^{1/2}$$

$$\text{where } \boldsymbol{\lambda}^{1/2} = \begin{bmatrix} \sqrt{\lambda_1} & \cdot & \cdot & \cdot & \cdot \\ \cdot & \cdot & \cdot & \cdot & \cdot \\ \cdot & \cdot & \cdot & \cdot & \cdot \\ \cdot & \cdot & \cdot & \cdot & \cdot \\ \cdot & \cdot & \cdot & \cdot & \sqrt{\lambda_n} \end{bmatrix} \tag{10}$$

The matrix $\mathbf{f}$ and vector $\mathbf{d}$ are then used in Eq. (4) to generate the disaggregated $\mathbf{y}(\mathbf{t})$.

The application of above statistical disaggregation procedure to the predicted annual rainfall of Figs. 5(a and b) yielded disaggregated rainfall totals shown in Figs. 7(a and b), respectively. The latter figures show that both disaggregated and observed rainfall at Ndola are characterized by bimodal peaks, one in December–January (DJ) and the other in February–March (FM). The DJ peak is associated with the southward passage of the

Downloaded 29 Dec 2010 to 160.36.192.127. Redistribution subject to ASCE license or copyright. Visit http://www.ascelibrary.org

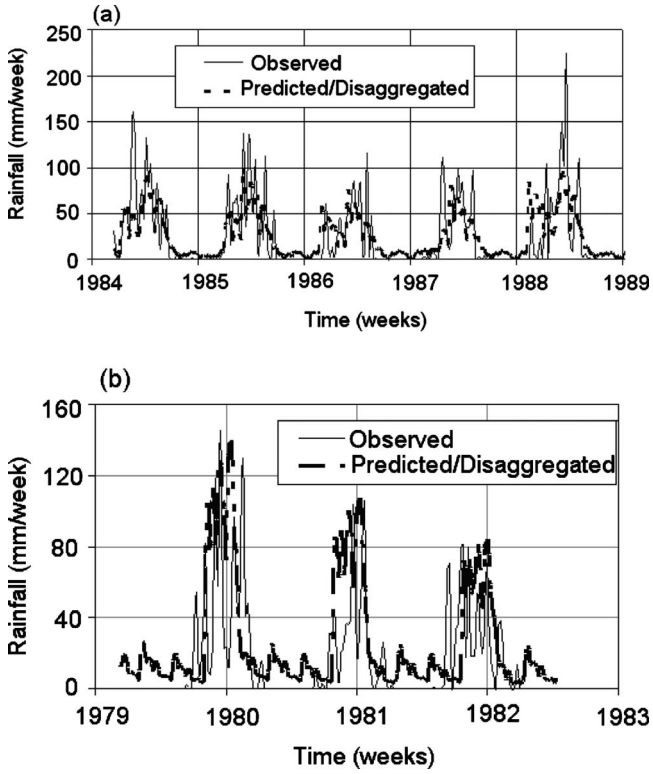

Fig. 7. Example showing disaggregated and observed weekly rainfall at (a) Ndola; (b) Solwezi

moist Congo-air front through Ndola while the FM peak is associated with the passage of the front during the northward displacement of the Congo air mass. The latter peak generally appears larger than the former. The general rainfall features associated with the intrusion (extrusion) of the Congo air mass in (out) of the Kafue basin appears to be captured by the distribution matrices d, while the matrix $\mathbf{f}$ adds a reasonable randomness (or "natural" look) to the weekly rainfall. The disaggregated weekly rainfall was then used to drive the Sacramento Soil Moisture Accounting model (SAC-SMA) (Burnash et al. 1973; Burnash 1995).

Hydrologic Model (SAC-SMA)

SAC-SMA was chosen because it only requires modest climatic data while physically-based hydrologic models are data-intensive, and climatic data are scarce in the Kafue River Basin. SAC-SMA is a lumped, deterministic conceptual model, made up of upper and lower conceptual storages, from which direct flow, Horton overland flow, interflow, subsurface flow, and evaporation are simulated. Soil moisture storages of the upper and lower zones are divided into free and tension water. The upper zone represents the top soils and the basin interception layers, while the lower zone represents the groundwater storage. As conceptual models, SAC-SMA requires the lumped parameters to be realistically calibrated by manual and automatic calibration procedures (Gan and Biftu 1996; Duan et al. 1992) in order to simulate runoff that matches the observed streamflow. Given that parameter values can vary over a wide range (e.g., 0–250 mm for the tension storages and 0–900 mm for the lower zone free water storages), the search for model parameters of global optimal quality can been tedious.

As one of the input data to SAC-SMA, potential evapotranspiration (ET) were estimated by the Complementary Relationship Areal Evapotranspiration (CRAE) model of Morton (1983), which has been recommended by Chiew and McMahon (1991), and Hobbins et al. (2001).

Estimation of Potential Evapotranspiration

The CRAE model assumes that when an area is getting drier, the actual ET decreases but the potential ET increases. CRAE assumes that the decrease in the actual ET generates an equal but opposite change in the potential ET, so that the sum of both equal to the maximum ET from a wet environment, represented as

$$E_T + E_{TP} = 2E_{TW} \tag{11}$$

where E_T=areal ET; E_{TP}=potential ET estimated from a solution of vapor transfer and energy balance equations; and E_{TW}=wet environment areal ET. According to CRAE, the actual ET resulting from feedbacks between the land surface and atmosphere interaction can be computed as

$$E_{Tw} = g_1 + g_2 \frac{\Delta_p}{\Delta_p + \gamma_p} R_n^* \tag{12}$$

where R_n^* is the net radiation adjusted to the equilibrium temperature T_p, Δp (mbar °C^{-1}) is the slope of the saturation vapor pressure at T_p, γ_p (mbar °C^{-1}) is the psychometric constant equal to 66.8 Pa/°C, g_1=14 Wm^{-2} (to account for large-scale advection during seasons of low or negative radiation and represents the minimum energy available for E_{Tw}), and g_2=1.2 is an empirical constant that Morton (1983) obtained through calibration. CRAE has been calibrated on a monthly basis and applied to diverse environments around the world, including Africa.

To estimate the potential ET in the CRAE model, average weekly temperature is needed for the following year. Weekly temperatures were estimated from monthly temperatures by simple averaging while monthly temperatures were estimated by simple averaging and a harmonic analysis defined as

$$w(t) = \hat{w}(t) + C_1 \cos\left(\frac{2\pi t}{n} - \Phi\right) + R(t) \tag{13}$$

where $w(t)$=predicted monthly temperature; $\hat{w}(t)$=average monthly temperature; C_1=constant; n=fundamental period (i.e., 12 months); t=time in months; Φ=phase shift in radians; and $R(t)$=random numbers ranging between −1 and 1, with a mean of zero and a variance of'1. $R(t)$ is included in Eq. (13) to include some stochastic processes observed in nature. Without $R(t)$, $w(t)$ will be a pure sine or cosine wave which may not appear natural, albeit monthly temperature generally exhibits sinusoidal behavior. As the amplitude of the harmonic function, C_1 is computed as

$$C_1 = \sqrt{A^2 + B^2}$$

$$\text{where } A = \frac{2}{n}\sum_{t=1}^{n} w(t)\cos\left(\frac{2\pi t}{n}\right) \text{ and } B = \frac{2}{n}\sum_{t=1}^{n} w(t)\sin\left(\frac{2\pi t}{n}\right) \tag{14a}$$

The phase shift, Φ, is then computed as

Downloaded 29 Dec 2010 to 160.36.192.127. Redistribution subject to ASCE license or copyright. Visit http://www.ascelibrary.org

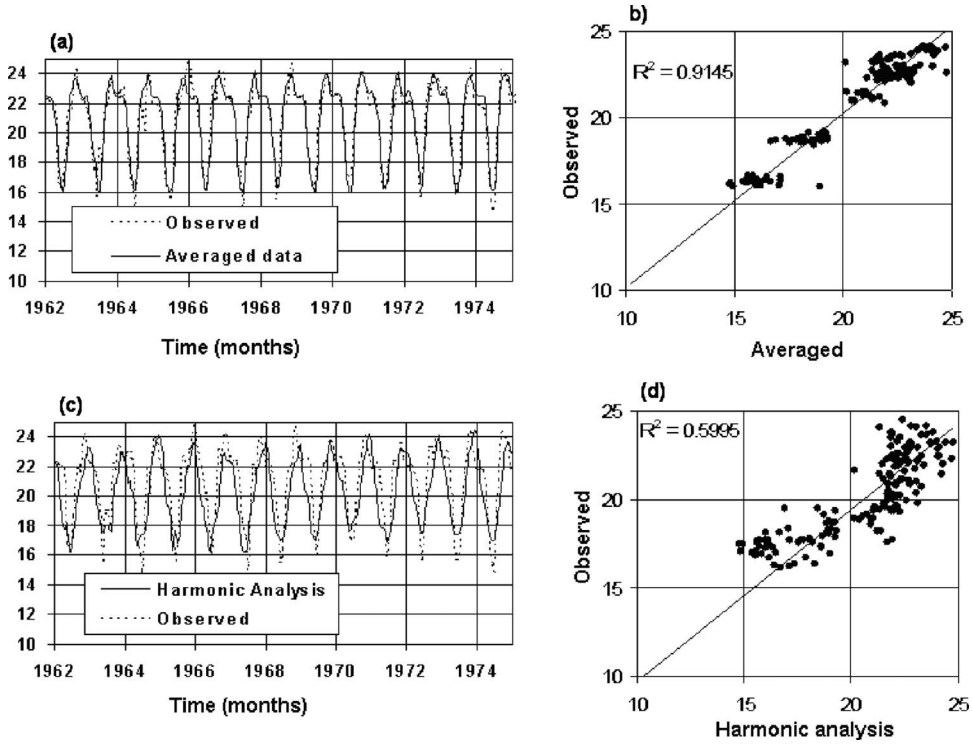

Fig. 8. Comparison of observed and predicted monthly air temperature (a) and (b) using simple averaging; and (c) and (d) using harmonic analysis

$$\Phi = \begin{cases} = \tan^{-1}\dfrac{B}{A} & A > 0 \\ = \tan^{-1}\dfrac{B}{A} \pm \pi & A < 0 \\ = \dfrac{\pi}{2} & A = 0 \end{cases} \tag{14b}$$

Using the averaging approach, the basin-wide averaged monthly temperatures were estimated as follows:

$$w(t) = \hat{W}(t) + T_r + R(t) \tag{15}$$

where $\hat{W}(t)$=vector of average monthly temperatures computed in a period; t=length of the training data; T_r is approximately the linear trend observed in the average monthly temperature data; and $R(t)$=random numbers as defined above.

Examples of predicted and observed air temperatures are shown in Fig. 8. Fig. 8(a) shows that air temperature estimated from simple averaging accounted for about 91% of variability of the observed air temperature, while Fig. 8(b) shows that Harmonic analysis only accounted for about 60% of the variability of the observed air temperature. Since the RMSE and biases were also higher for the air temperature estimated by Harmonic analysis, the air temperature data from the simple averaging approach was chosen for this study.

Discussion of Results

Prediction Skill

The prediction skill was assessed in terms of the Nash-Sutcliffe coefficient of efficiency (E_f), the bias, root-mean-square error (RMSE) and the Pearson correlation (Corr) as follows:

$$E_f = 1 - \frac{\sum_{i=1}^{K}(X_i - O)^2}{\sum_{i=1}^{K}(X_i - \bar{X})^2} \tag{16}$$

$$\text{Bias} = \frac{1}{K}\sum_{i=1}^{K}(X_i - O_i) \tag{17}$$

$$\text{RMSE} = \frac{1}{K}\sqrt{\sum_{i=1}^{K}(X_i - O_i)^2} \tag{18}$$

$$\text{Corr} = \frac{1}{K}\frac{\sum_{i=1}^{K}(X_i - \bar{X})(O_i - \bar{O})}{\sqrt{\sum_{i=1}^{K}(X_i - \bar{X})^2 \sum_{i=1}^{K}(O_i - \bar{O})^2}} \tag{19}$$

where O_i and X_i=observed and modeled streamflow discharges respectively; $\bar{X}$ and $\bar{O}$ are their respective mean values; and K=total number of observed O_i and X_i values. The Pearson correlation ranges from −1 to 1 with a correlation of 1 (−1) being a perfect linear positive (negative) relationship between O_i and X_i, and a correlation of zero indicating no relationship between O_i and X_i, while the Nash-Sutcliffe coefficient efficiency may range from −∞ to 1, with an efficiency of 1 corresponding to a perfect match, an efficiency of 0 indicating model predictions that are only as good as the mean of O_i, and an efficiency less than zero indicating that the prediction is as good as random.

Downloaded 29 Dec 2010 to 160.36.192.127. Redistribution subject to ASCE license or copyright. Visit http://www.ascelibrary.org

Table 1. Summary Statistics of Statistically Disaggregated Weekly Rainfall at Ndola

Year	1984	1985	1986	1987	1988	Average
Explained variance (R^2 as %)	59	56	47	51	34	49.
RMSE (mm/week)	29	25	21	23	39	27
BIAS (mm/week)	−6	−1	3	−2	2	−0.8
Efficient coefficient (E_f)	0.53	0.57	0.46	0.49	0.33	0.46

Skill of Predicted Rainfall

The observed and predicted annual rainfall shown in Fig. 5(a) has a Pearson correlation of 0.98, E_f of 0.88, RMSE of 31.2 mm and Bias of 22.1 mm, while that of Fig. 5(b) has a Pearson correlation of 0.99, E_f of 0.92, RMSE of 24.2 mm, bias of 22.3 mm. From these statistics, it is clear that the ANN-GA model exhibited a high prediction skill and predicted the annual rainfall very accurately.

The prediction skills of statistically disaggregated weekly rainfall at Ndola and Solwezi are shown in Tables 1 and 2, respectively. Table 1 shows that disaggregated rainfall at Ndola accounted for between 47 and 59% of the observed weekly rainfall variability, while RMSE ranged between 21 mm to 39 mm/week, biases −6 to 3 mm and E_f from 0.33 to 0.57. Table 2 shows that at Solwezi, disaggregated rainfall accounted for between 23% and 35% of the observed weekly rainfall variance, with RMSEs ranging from 25 mm to 45 mm/week, biases of 4 to 10 mm and E_f of −0.22 to 0.05. The above statistics clearly indicate that disaggregating rainfall at Solwezi is much more challenging than at Ndola. The difference is most likely associated with the strength of the rainfall signal at the two stations, with Ndola having a stronger rainfall signal because it lies in the middle of the upper Kafue basin, while Solwezi is located near the outskirts of the river basin [see Fig. 3(a)]. Using the 336 weeks of observations between 1962 and 1968, a correlation of 0.10 (or 10%) is statistically significant at the 95% level. Hence, although the prediction skill does not appear to be strong, the explained variance of greater than 10% means that the predicted rainfall generally captured the variability of weekly rainfall.

Skill of Predicted Runoff

For the upper Kafue River Basin, SAC-SMA was calibrated using the 1962–1983 weekly rainfall and runoff data and validated using the 1984–1988 data. For the Lunga basin, calibration was performed using the 1962–1979 rainfall and runoff data and validated using the 1980–82 data. In this study, SAC-SMA was set to perform soil moisture accounting operations at weekly time step. However, internally SAC-SMA accounts for soil moisture distribution between the free and tension storages of the upper and lower zones in much smaller time increments, the generation of surface and subsurface flows, and the evapotranspiration (ET). At the end of each time period, the net channel inflow was essentially the total precipitation input minus ET and the net moisture assigned to the storage zones.

Table 2. Summary Statistics of Statistically Disaggregated Weekly Rainfall at Solwezi

Year	1980	1981	1982	Average
Explained variance (R^2 as %)	23	35	27	23
RMSE (mm/week)	41	29	25	32
BIAS (mm/week)	10	13	4	9
Efficient coefficient (E_f)	−0.22	−.33	0.05	−0.17

Performance of SAC-SMA for the Upper Kafue River Basin

The performance of SAC-SMA for the Kafue River Basin, for each of the five years between 1984 and 1988, using both historical and disaggregated weekly rainfall at Ndola is shown in Figs. 9(a and b). Historical weekly rainfall at Ndola was used as a benchmark to assess the performance of SAC-SMA when it was driven by disaggregated weekly rainfall. The summary statistics corresponding to Figs. 9(a and b) are presented in Tables 3 and 4, respectively. Table 3 shows that when historical weekly rainfall data was used, on an annual basis the explained variance between observed and simulated runoff ranged between 81 and 95%, RMSE ranged between 37 and 95 mm/week, biases ranged between −54 to 14 mm and E_f ranged between 0.82 and 0.95. On the other hand, when disaggregated weekly rainfall was used, the explained variance between observed and simulated runoff ranged between 78 and 90%, RMSE ranged between 37 and 92 mm/week, biases ranged between −36 to 14 mm and E_f ranged between 0.71 and 0.95. Apparently, the performance of SAC-SMA

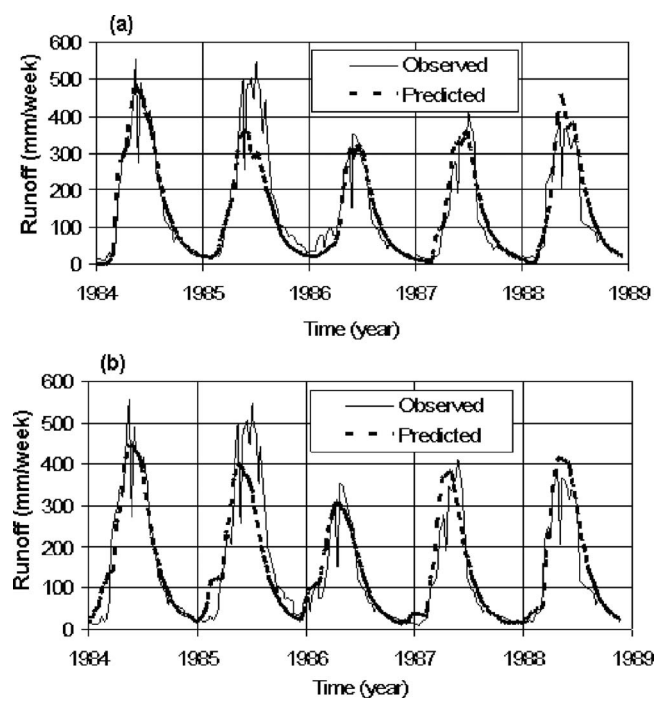

Fig. 9. Observed and predicted weekly streamflow (m^3/s) for the Kafue River Basin using (a) observed weekly rainfall; (b) statistically predicted weekly rainfall

Downloaded 29 Dec 2010 to 160.36.192.127. Redistribution subject to ASCE license or copyright. Visit http://www.ascelibrary.org

Table 3. Summary Statistics of SAC-SMA's Prediction Skill Using Historical Weekly Rainfall for the Upper Kafue Basin

Year	1984	1985	1986	1987	1988	Average
Explained variance (R^2 as %)	95	81	87	89	87	88
RMSE (mm/week)	37	95	38	41	55	53
BIAS (mm/week)	4	−54	−6	9	14	−8
Efficient coefficient (E_f)	0.95	0.70	0.85	0.89	0.82	0.84

Table 4. Summary Statistics of SAC-SMA's Prediction Skill Using Statistically Generated Weekly Rainfall for the Upper Kafue Basin

Year	1984	1985	1986	1987	1988	Average
Explained variance (R^2 as %)	90	78	87	82	88	85
RMSE (mm/week)	51	92	37	54	51	57
BIAS (mm/week)	−2	−36	8	12	14	−0.8
Efficient coefficient (E_f)	0.90	0.71	0.87	0.80	0.85	0.83

only depends marginally on whether disaggregated or historical weekly rainfall was used. This likely shows that with weekly rainfall disaggregated from the annual rainfall predicted by the ANN-GA, SAC-SMA can generally predict the weekly streamflow for the upper Kafue basin accurately.

Performance of the SAC-SMA for the Lunga River Basin

Due to a lack of data, only three years (1980–1982) were used for validating this sub-catchment and the validation results using both historical and disaggregated rainfall are shown in Figs. 10(a and b) and in Tables 5 and 6, respectively. Table 5 shows that the explained variances between the predicted and observed weekly streamflow ranged between 72 and 90%, RMSE ranged from 15 to 85 mm/week, biases from −28 to 7 mm/week, and E_f from 0.50 to 0.90. On the other hand, Table 6 shows that the explained variances between the predicted and observed weekly streamflow ranged between 61 and 84%, RMSE ranged from 15 to 86 mm/week, biases from −28 to 7 mm/week, and E_f from 0.50 to 0.83. In both cases, the high flows could not be predicted accurately. Apparently the difference in the accuracy of simulated streamflow based on observed and disaggregated weekly rainfall is marginal.

The prediction skill is generally modest because SAC-SMA failed to simulate peak streamflows partly because as a lumped-parameter model, SAC-SMA could not account for the distributed nature of Lunga's hydrologic processes. Furthermore, it could be because model parameters for the upper and lower water zones were much higher than those suggested in previous studies, peak flows tend to be under-simulated.

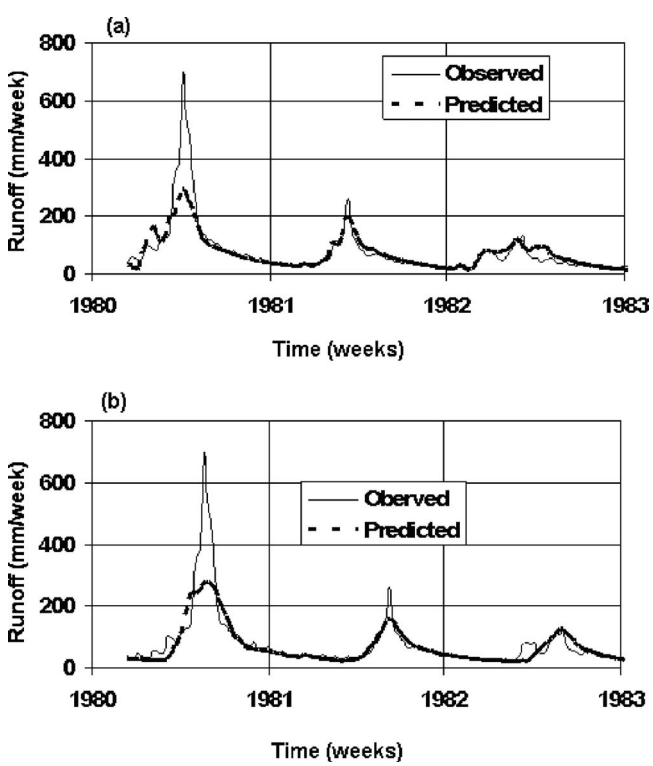

Fig. 10. Observed and predicted weekly streamflow (m^3/s) of the Lunga River Basin using (a) observed rainfall; (b) statistically predicted rainfall

SAC-SMA Model Parameters

Table 7 shows the optimized parameters of the upper Kafue and Lunga River Basins, calibrated through a combination of manual and the global optimization algorithm of Duan et al. (1992). Fig. 11 shows an example run of how model parameters got optimized in the optimization process. Using the above procedure, the upper zone tension moisture capacity and the free water storages of these two basins were found to be 382–388 and 299 mm, respectively, which were much higher than the upper

Table 5. Summary Statistics of SAC-SMA's Prediction Skill Using Historical Weekly Rainfall for the Lunga River Basin

Year	1980	1981	1982	Average
Explained variance (R^2 as %)	80	90	72	81
RMSE (mm/week)	85	15	19	40
BIAS (mm/week)	−28	2	7	−6
Efficient coefficient (E_f)	0.63	0.90	0.50	0.7

Table 6. Summary Statistics of SAC-SMA Prediction Skill Using the Statistically Generated Weekly Rainfall for the Lunga River Basin

Year	1980	1981	1982	Average
Explained variance (R^2 as %)	72	84	61	72
RMSE (mm/week)	86	18	19	41
BIAS (mm/week)	−28	−3	−0.1	−10
Efficient coefficient (E_f)	0.62	0.83	0.50	0.65

Downloaded 29 Dec 2010 to 160.36.192.127. Redistribution subject to ASCE license or copyright. Visit http://www.ascelibrary.org

Table 7. Optimal Parameters for the Kafue and Lunga River Basins

Parameter	Kafue optimized parameters (mm)	Lunga optimized parameters (mm)	Parameter definition
UZTWM	382	388	Upper zone tension water
UZFWM	299	299	Upper zone free water capacity
UZK	0.06	0.06	Upper zone withdrawal rate
ZPERC	28	24	Maximum percolation rate
REXP	1.001	1.026	Exponent for the percolation equation
LZTWM	300	253	Lower zone tension water
LZFSM	345	328	Lower zone free water capacity

limits suggested by Gan and Burges (1990a, b) (i.e., 5–250 and 3–30 mm, respectively). These values were found via automatic calibration, by starting off with initial parameter values of 29 and 15 mm, respectively. The difference could be partly because the bounds recommended by Gan and Burges (1990a, 1990b) were mainly based on North American experience. These large upper storages probably reflect the high storage capacity attributed to the dominance of numerous dambos, clays, and sandveldt soils. The lower zone parameters are within the bounds suggested by Gan and Burges (1990a, 1990b) but again suggesting that the basins might have relatively large lower zone storage capacity. The large storage parameters especially that of the upper zones partly explain why the peak runoff was under simulated, and also possibly due to uncertainties associated with observed rainfall data collected by a limited number of rain gauges.

Even though the parameters derived by the global search routine of Duan et al. (1992) should be of global optimum quality, SAC-SMA is still a lumped-parameter, conceptual hydrologic model that ignores the spatial variation of basin characteristics (e.g., soil properties, terrain, vegetation) and climate data, that conceptualizes the essential basin-scale hydrologic processes with a model structure that is a simplified version of nature which is highly heterogeneous and complex. Therefore predicting the basin streamflow by this pragmatic but simplified system inevitably involves a certain degree of uncertainties.

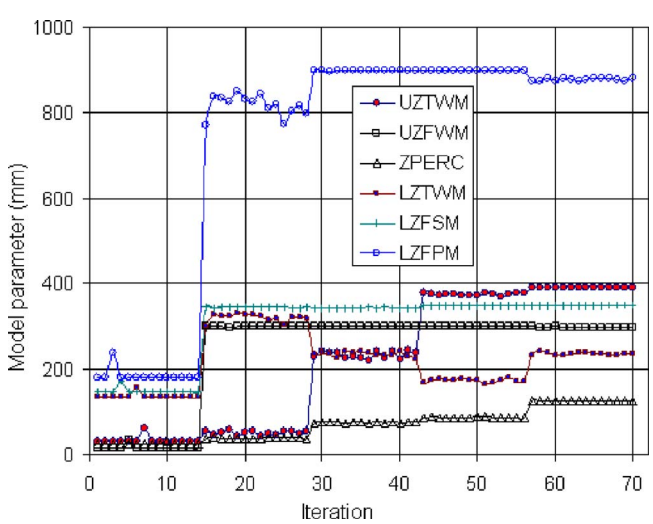

Fig. 11. Automated calibration run showing the evolution of the upper and lower zone model parameters

Summary and Conclusions

This paper developed a framework to integrate wavelet empirical orthogonal function analysis, artificial neural networks driven by a genetic algorithm, statistical disaggregation and a lumped parameter hydrologic model to predict weekly rainfall and runoff for the Kafue and Lunga River Basins in Zambia, Africa. Results show that predicted and statistically disaggregated rainfall explained about 47% of observed rainfall at Ndola (upper Kafue basin) and 23% at Solwezi. Using this weekly rainfall, the simulated runoff for the upper Kafue and Lunga Rivers accounted for 81% and 72% of the variance of the observed runoff, respectively, compared to 88% and 81% when historical weekly rainfall were used.

The results generally show that statistical properties of hydroclimatic process at Kafue and Lunga River Basins are approximately stationary, and so statistically generated rainfall may be used to predict the basin runoff with considerable skill. Since the weekly streamflow can be predicted at least at three months up to a year lead time, this procedure can be used to provide reliable estimates of weekly runoff for the upper Kafue basin at Iteshi-Teshi reservoir which could be useful for integrated water resources management, especially during years of low rainfall or drought.

Acknowledgments

This project was partly funded by the Natural Science and Engineering Research Council of Canada. The first writer was also partly funded by the Sustainable Forest Management Fund of Canada.

Notation

The following symbols are used in this paper:

a = scale (or periodic cycle) of the wavelet;
b = translation position along the t-axis of a wavelet transformation;
C_1 = amplitude of the harmonic function;
C_δ = constant equal to 0.776;
$\mathbf{d}$ = vector of coefficients;
E_f = Nash-Sutcliffe coefficient efficiency;
E_T = areal evapotranspiration;
E_{TP} = potential evapotranspiration;
E_{TW} = wet environment areal evapotranspiration;
e = eigenvectors;
$\mathbf{f}$ = matrix of coefficients;
g_1 = empirical constant=14 Wm^{-2};
g_2 = empirical constant=1.2;
M = number of dominant WPCs;
O = observed rainfall, streamflow or SST time series;
$\bar{O}$ = mean of observed rainfall, streamflow or SST time series;
R_n^* = net radiation;
R = random numbers ranging between −1 and 1;
s_{yx} = covariance matrices;
T_p = equilibrium temperature;
T_r = approximation of the linear trend observed in the average monthly temperature data;
T_r = wavelet principle components (WPCs) time series;
$v(t)$ = vector of random standard normal deviates;

Downloaded 29 Dec 2010 to 160.36.192.127. Redistribution subject to ASCE license or copyright. Visit http://www.ascelibrary.org

$\hat{W}(t)$ = vector of average monthly temperatures;
$w(t)$ = predicted monthly temperature;
$\hat{w}(t)$ = average monthly temperature;
X_i = modeled streamflow discharges;
$\bar{X}$ = mean modeled streamflow discharges;
$x(t)$ = annual or seasonal rainfall;
x'_k = anomalies of the SAWP;
$y(t)$ = vector of monthly or weekly rainfall totals;
δ_j = factor for scale averaging;
δ_t = sampling period;
Δ_p = slope of the saturation;
ψ = mother wavelet;
λ_i = eigen values;
γ_p = psychometric constant equal to 66.8 Pa/ °C; and
Φ = phase shift in radians.

References

Bindlish, R., and Barros, A. (2000). "Disaggregation of rainfall for one-way coupling of atmospheric and hydrological models in regions of complex terrain." *Glob. Planet. Change*, 25, 111–132.

Burnash, R. J., Ferral, R. L., and Maguire, R. A. (1973). "A generalized streamflow simulation system." *Conceptual modeling for digital computers*, National Weather Service, Sacramento, CA.

Burnash, R. J. C. (1995). "The NWS river forecast system—Catchment modeling." *Computer models of watershed hydrology*, V. P. Singh, ed., 311–366.

Chiew, F. H. S., and McMahon, T. A. (1991). "The applicability of Morton and Penman's evaporation estimates in rainfall-runoff modeling." *Water Resour. Res.*, 27, 611–620.

Chow, V. T., Maidment, D. R., and Mays, L. M. (1988). *Applied hydrology*, McGraw-Hill.

Duan, Q., Sorooshian, S., and Gupta, V. (1992). "Effective and efficient global optimization for conceptual rainfall-runoff models." *Water Resour. Res.*, 28, 1015–1031.

Fanta, B., Zaake, B. T., and Kachroo, R. K. (2001). "A study of the variability of the river flow of the southern Africa region." *Hydrol. Sci. J.*, 46, 513–524.

Gan, T. Y., and Biftu, G. F. (1996). "Automatic calibration of conceptual rainfall-runoff models: Optimization algorithms, catchment conditions, and model structure." *Water Resour. Res.*, 32(12), 3513–3524

Gan, T. Y., and Burges, S. J. (1990a). "An assessment of a conceptual rainfall-runoff model's ability to represent the dynamics of small hypothetical catchments. 1: Model, model properties, and experimental design." *Water Resour. Res.*, 26(7), 1595–1604.

Gan, T. Y., and Burges, S. J. (1990b). "An assessment of a conceptual rainfall-runoff model's ability to represent the dynamics of small hypothetical catchments. 2: Hydrologic responses for normal and extreme rainfall." *Water Resour. Res.*, 26(7), 1605–1619.

Hobbins, M. T., Ramirez, J. A., Brown, T. C., and Claessens, L. H. M. (2001). "The complementary relationship in estimation of regional evapotranspiration: The complementary relationship areal evaporation and advection-aridity models." *Water Resour. Res.*, 37, 1367–1387.

Jury, M. R., and Engert, S. (1999). "Teleconnections modulating interannual climate variability over northern Namibia." *Int. J. Climatol.*, 19, 1459–1475.

Kerkhoven, E., and Gan, T. Y. (2006). "A modified ISBA surface scheme for modeling the hydrology of Athabasca River Basin with GCM-scale data." *Adv. Water Resour.*, 29(6), 808–826.

Lorenz, E. N. (1969). "Atmospheric predictability as revealed by naturally occurring analogs." *J. Atmos. Sci.*, 26, 636–646.

Morton, F. I. (1983). "Operational estimates of actual evapotranspiration and their significance to the science and practice of hydrology." *J. Hydrol.*, 66, 1–76.

Mwale, D., and Gan, T. Y. (2005). "Wavelet analysis on variability, teleconnectivity and predictability of the September-November East African rainfall." *J. Appl. Meteorol.*, 44, 256–269.

Mwale, D., Gan, T. Y., and Shen, S. P. (2004). "A new analysis of variability, teleconnectivity and predictability of rainfall of central southern Africa, 1950–1994." *Int. J. Climatol.*, 24, 1509–1530.

Mwale, D., Gan, T. Y., Shen, S. P., Shu, T. T., and Kim, K.-M. (2007). "Wavelet empirical orthogonal functions of space-time-frequency regimes and predictability of southern Africa summer rainfall." *J. Hydrol. Eng.*, 12(5), 513–523.

New, et al. (2002). SAFARI 2000 project, ⟨http://www.daac.ornl.gov⟩.

Peitgen, H.-O., Jurgens, H., and Saupe, D. (1992). *Chaos and fractals—New frontiers of science*, Springer.

Torrence, C., and Compo, G. P. (1998). "A practical guide to wavelet analysis." *Bull. Am. Meteorol. Soc.*, 79, 61–78.

United Nations Development Planning/Food and Agricultural Organization/Government of the Republic of Zambia (UNDP/FAO/GRZ). (1968). "Multipurpose survey of the Kafue River Basin, Zambia, Vol. III, Climatology and hydrology." *Rep. No. FAO/SF; 35/ZAM*.

Valencia, R. D., and Schaake, J. C. (1972). *A disaggregation model for time series analysis and synthesis, Report 149, Ralph M. Parsons Lab, for water resources and hydrodynamics*, Massachusetts Institute of Technology, Cambridge, MA.

Valencia, R. D., and Schaake, J. C. (1973). "Disaggregation process in stochastic hydrology." *Water Resour. Res.*, 9, 580–585.

The Water Page. (2005). ⟨http://www.thewaterpage.com/IWRM_Zimbabwe.htm⟩.

Yarnal, B., Lakhtakia, M. N., Yu, Z., White, R. A., Pollard, D., Miller, D. A., and Lapenta, W. M. (2000). "A linked meteorological model system: The Susquehanna River Basin experiment (SRBEX)." *Glob. Planet. Change*, 25, 149–161.

Downloaded 29 Dec 2010 to 160.36.192.127. Redistribution subject to ASCE license or copyright. Visit http://www.ascelibrary.org